Biosensors and Bioelectronics 33 (2012) 44–49

Contents lists available at SciVerse ScienceDirect

Biosensors and Bioelectronics

journal homepage: www.elsevier.com/locate/bios

Amperometric acetylcholine biosensor based on self-assembly of gold nanoparticles and acetylcholinesterase on the sol–gel/multi-walled carbon nanotubes/choline oxidase composite-modified platinum electrode

Shihua Hou [a], Zhongmin Ou [b], Qiang Chen [c], Baoyan Wu [b,*]

[a] School of Electronic and Information Engineering, South China University of Technology, Guangzhou 510641, China
[b] MOE Key Laboratory of Laser Life Science & Institute of Laser Life Science, College of Biophotonics, South China Normal University, Guangzhou 510631, China
[c] The Key Laboratory of Bioactive Materials Ministry of Education, College of Life Sciences, Nankai University, Tianjin 300071, China

ARTICLE INFO

Article history:
Received 2 September 2011
Received in revised form 7 December 2011
Accepted 8 December 2011
Available online 16 December 2011

Keywords:
Layer-by-layer
Sol–gel
Carbon nanotubes
Gold nanoparticles
Acetylcholine biosensor

ABSTRACT

A novel acetylcholinesterase (AChE)/choline oxidase (ChOx) bienzyme amperometric acetylcholine biosensor based on gold nanoparticles (AuNPs) and multi-walled carbon nanotubes (MWCNTs) has been successfully developed by self-assembly process in combination of sol–gel technique. A thiolated aqueous silica sol containing MWCNTs and ChOx was first dropped on the surface of a cleaned Pt electrode, and then AuNPs were assembled with the thiolated sol–gel network. Finally, the alternate deposition of poly (diallyldimethylammonium chloride) (PDDA) and AChE was repeated to assemble different layers of PDDA-AChE on the electrode for optimizing AChE loading. Among the resulting biosensors, the biosensor based on two layers of PDDA-AChE multilayer films showed the best performance. It exhibited a wide linear range, high sensitivity and fast amperometric response, which were 0.005–0.4 mM, 3.395 μA/mM, and within 15 s, respectively. The biosensor showed long-term stability and acceptable reproducibility. More importantly, this study could provide a simple and effective multienzyme immobilization platform for meeting the demand of the effective immobilization enzyme on the electrode surface.

1. Introduction

The development of the acetylcholinesterase (AChE)-based biosensor is of crucial importance for healthy inspection and environment protection. Firstly, acetylcholine is one of the first neurotransmitters discovered in the brain and the peripheral nervous system and it plays numerous roles (Liu et al., 2005). Determination of acetylcholine is important for the characterization of cholinergic transmission in normal and pathological physiology (Mitchell, 2004), which is of major importance in biotechnology as well as in clinical applications (Ozturk et al., 2007). In addition, AChE is the most important target molecule of organophosphates compounds which are known as inhibitors of AChE. Therefore, many AChE-based biosensors have been proposed via electrochemiluminescence (Wang et al., 2009; Deng et al., 2011), fluorescence (Ozturk et al., 2007; Chen et al., 2011), and amperometric methods (Pchelintsev and Millner, 2008; Vamvakaki et al., 2008; Shimomura et al., 2009; Zhu et al., 2009). Among AChE-based biosensors, the amperometric AChE/choline oxidase (ChOx) bienzyme-based biosensor is especially promising because of its potential high sensitivity, good selectivity and reproducibility. The working mechanism of AChE/ChOx bienzyme biosensor for acetylcholine is based on the following sequential biochemical reactions (Chen et al., 1998):

$$\text{acetylcholine} + H_2O \xrightarrow{\text{AChE}} \text{choline} + \text{acetate}$$

$$\text{choline} + H_2O + 2O_2 \xrightarrow{\text{ChOx}} \text{betaine} + 2H_2O_2$$

In the presence of oxygen, AChE and ChOx catalyze the successive reactions of acetylcholine to form hydrogen peroxide (H_2O_2) which can be easily oxidized at an electrode. The oxidation current of hydrogen peroxide can be used as a measure of acetylcholine, choline and AChE activity.

The key aspect in developing any enzyme-based biosensors is the effective immobilization of enzyme on the solid electrode surface (Yang et al., 2005; Wu et al., 2007a). One another important criterion for the performance of this bienzyme biosensor is the ratio of the two enzymes present on the electrode surface (Mackey et al., 2007). Compared to one enzyme, bienzyme immobilization is more complex. It is highly desired to develop a simple and effective AChE/ChOx bienzyme immobilization matrix for

* Corresponding author. Tel.: +86 20 85217070; fax: +86 20 85216052.
E-mail address: wubaoyan@scnu.edu.cn (B. Wu).

0956-5663/$ – see front matter © 2011 Elsevier B.V. All rights reserved.
doi:10.1016/j.bios.2011.12.014

fabricating the high biological activity and stability of acetylcholine biosensor.

Since Wang et al. (1998b) firstly proposed a simple and attractive procedure for the design of three-dimensional silica gel network based on the coupling of self-assembled monolayer and sol–gel process, this procedure has attracted much attention. It has been demonstrated that the coupling of sol–gel and self-assembly process is an effective and versatile method for immobilization of a variety of biomolecules (Shen et al., 2005). One of the quality examples was the fabrication of a third-generation horseradish peroxidase amperometric biosensor developed by self-assembling gold nanoparticles (AuNPs) to a thiol-containing sol–gel network (Jia et al., 2002). In view of the fact that AuNPs can assist the electron transfer, the resulting biosensor exhibited high sensitivity, good reproducibility, and long-term stability. AuNPs are the promising nanomaterials explored for chemical and biological sensing application, because AuNPs are suitable for binding of biomolecules due to facilitation of direct and fast electron transfer (Andreescu and Luck, 2008; Huang et al., 2011). Therefore, the combination of this procedure and AuNPs has attracted wide attention for use in different types of biosensors. For example, Deng et al. (2009) provided a new biocompatible platform for constructing the dehydrogenase-based electrochemiluminescence biosensor based on sol–gel and AuNPs. Recently, Kannan and Abraham John (2010) reported a hydroxylamine amperometric biosensor using self-assembled AuNPs on sol–gel film, which showed good electrocatalytic properties.

Meanwhile, carbon nanotubes (CNTs) have also been demonstrated to provide an ideal platform for biosensing applications, which could possess advantages including their unique structures, a large edge/basal plane ratio, enhanced electronic properties, and rapid electrode kinetics (Zhang et al., 2009; Firdoz et al., 2010; Li et al., 2011). AuNP-CNTs nanostructures were successfully used to enhance the sensitivity of biosensors, which has attracted considerable attention in recent work. Previously, we reported an amperometric glucose biosensor based on self-assembly of multilayer films composed of multi-walled carbon nanotubes (MWCNTs), AuNPs and glucose oxidase for the specific detection of glucose. Compared with MWCNTs or AuNPs sensor, the electrochemical characteristics of MWCNTs/AuNPs-based sensor were much more improved (Wu et al., 2007b). Xiao et al. (2008) developed a biosensor for highly sensitive electrochemical detection of arsenic using AuNPs modified CNTs via anodic stripping voltammetry. More recently, Pundir et al. (2011) developed an amperometric oxalate biosensor using nanohybrid film of CNTs and AuNPs via carbodiimide chemistry, and found that the modified electrode exhibited a variety of good electrochemical characteristics including high sensitivity, rapid response and long-term stability. The hybrid nanostructures may improve the performances of the single component, and even extend the possible uses for these new composites (Tello et al., 2008; Minati et al., 2010).

Based on the above consideration, here we utilized the coupling of sol–gel and self-assembly process to fabricate a novel bienzyme amperometric acetylcholine biosensor based on MWCNTs and AuNPs in order to develop a simple and effective bienzyme immobilization matrix for meeting the demand of the effective immobilization enzyme on the electrode surface. To the best of our knowledge, self-assembly of AuNPs and AChE on the MWCNTs/ChOx/sol–gel modified electrode for constructing the bienzyme acetylcholine biosensor has not yet been reported.

The resulting biosensor should not only exhibit the benefits of the advantages of sol–gel, self-assembly, MWCNTs and AuNPs, but also can provide a universal and effective immobilization platform for constructing the multienzyme-based biosensor.

2. Experimental

2.1. Reagents

Acetylcholinesterase (AChE, EC3.1.1.7, 1100 units/mg protein, from electric eel), choline oxidase (EC1.1.3.17, 17 units/mg protein, from alcaligenes species), acetylcholine chloride, choline chloride, and (3-mercaptopropyl)trimethoxy silane (MPTMOS) were purchased from Sigma–Aldrich. MWCNTs (>50 nm diameter, length 0.5–2 μm, and >95% purity) were obtained from Chengdu Institute of Organic Chemistry, Chinese Academy of Science (China). Chloroauric acid hydrated ($HAuCl_4{\cdot}4H_2O$) was purchased from Sinopharm Chemical Reagent Co. (China). All the reagents were of analytical grade and used without further purification. The high-purity deionized water (resistance, 18 MΩ cm) was used throughout this work. Phosphate-buffered saline (PBS, pH 8.0) buffer was employed as supporting electrolyte. All experiments were performed in PBS at room temperature, approximately 25 °C.

2.2. Apparatus and measurements

Electrochemical measurements were carried out by a Potentiostat–Galvanostat (EG&G PARC Model 283 with a software M270). A three-electrode system was employed with the enzyme modified Pt electrode as the working electrode, a Pt wire as the auxiliary electrode and Ag/AgCl (saturated KCl) as the reference electrode in an electrochemical cell filled with 20 ml of PBS at room temperature. The electrochemical impedance spectroscopy (EIS) experiment was performed with a CHI660c electrochemical working station in 0.1 M KCl containing 5 mM $[Fe(CN)_6]^{3-/4-}$ (1:1) with a frequency range from 100 kHz to 1 Hz with an amplitude of 5 mV. The absorption spectrum of AuNPs was obtained using a UV/VIS spectrometer (Lambda 35, Perkin-Elmer, USA). To examine the size of AuNPs, the sample was observed by a JEM-2100HR transmission electron microscopy (TEM) at 200 kV.

2.3. Preparation of biosensor

2.3.1. Preparation of AuNPs and PDDA-MWCNTs

All glassware used in the following procedure was cleaned in a bath of freshly prepared solution (3:1 HNO_3–HCl), thoroughly washed with water, and dried prior to use. AuNPs were prepared according to the literature (Hill and Mikin, 2006) by adding sodium citrate to a boiling $HAuCl_4$ aqueous solution. The solution was kept boiling for 15 min under vigorous stirring, then allowed to cool down to room temperature, and stored at 4 °C.

MWCNTs were sonicated in PDDA solution (2 g/l), and centrifuged at 10,000 rpm for 10 min. The sediment comprising of impurities, aggregates, and bundles of nanotubes at the bottom of the centrifuge tube was discarded, and the supernatant containing PDDA-MWCNTs was collected.

2.3.2. Preparation of thiolated aqueous silica sol

Aqueous silica sol was prepared according to the literatures (Wang et al., 1998a; Jia et al., 2002). Briefly, MPTMOS with water at a 1:4 ratio, 10% of ethanol, and 3.3% of 0.1 M hydrochloric acid were mixed and sonicated for 30 min until a clear and homogenous solution resulted and was subsequently stored at room temperature for 2–3 h.

2.3.3. Configuration of the acetylcholine biosensor

The acetylcholine biosensor was prepared according to the following steps:

Step 1: the bare Pt electrode was polished with chamois leather containing 0.05 μm alumina slurry, rinsed thoroughly with water,

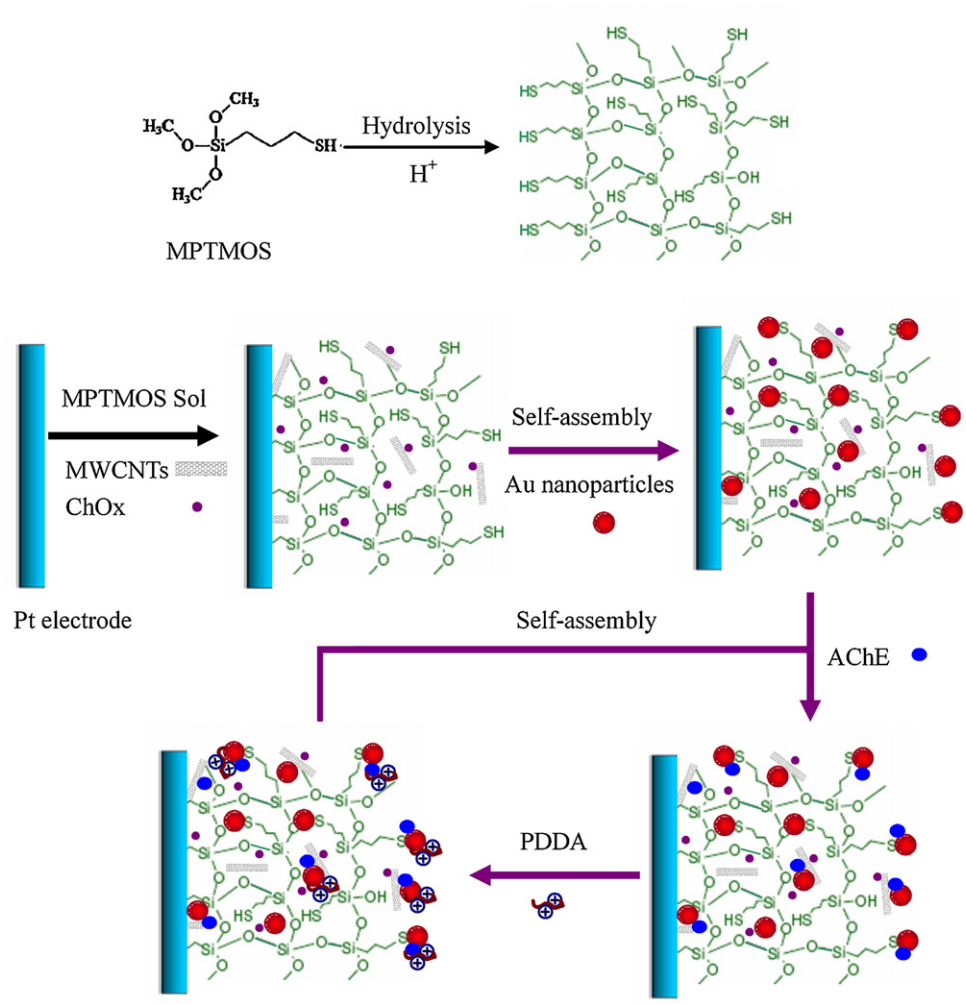

Fig. 1. Scheme of preparation of the AChE/ChOx bienzyme amperometric biosensor for acetylcholine based on MWCNTs and AuNPs using the coupling of sol–gel and self-assembly process.

successively sonicated in water and absolute ethanol, and dried at room temperature.

Step 2: a homogeneous stock sol–gel/MWCNTs/ChOx solution was prepared by carefully mixing sol–gel with ChOx (5 g/l) and PDDA-MWCNTs at a 1:4:2 volume ratio. Then the freshly mixture was dropped on the surface of Pt electrode, and allowed to dry at 4 °C, which was regarded as MWCNT-ChOx/Pt electrode.

Step 3: MWCNT-ChOx/Pt electrode was immersed in AuNPs solution for 5 h at 4 °C, and thoroughly rinsed with PBS which was applied at the end of each assembly deposition for dissociating the weak adsorption, which was regarded as MWCNT-AuNP-ChOx/Pt electrode.

Step 4: MWCNT-AuNP-ChOx/Pt electrode was alternately immersed in AChE (0.2 g/l) and PDDA solution according to the reported procedure (Shi et al., 2005). Briefly, MWCNT-AuNP-ChOx/Pt electrode was firstly immersed in AChE solution for 30 min to immobilize AChE, and then transferred to PDDA solution for 30 min. The alternate deposition of PDDA and AChE was repeated to assemble different layers of PDDA-AChE for optimizing AChE loading, which was regarded as MWCNT-AuNP-(PDDA-AChE)n/Pt electrode.

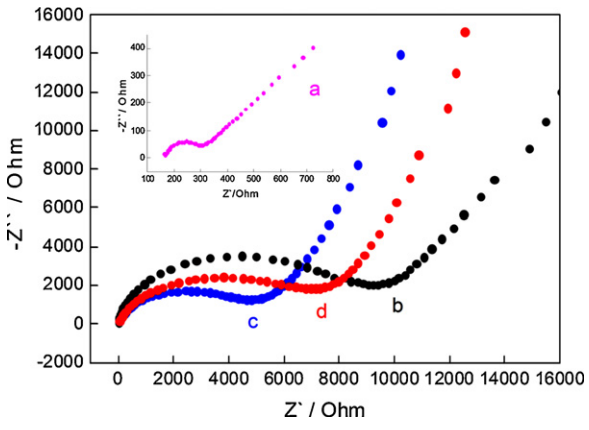

Fig. 2. Electrochemical impedance spectroscopy of the bare electrode (a), sol-MWCNTs/Pt (b), sol-MWCNT-AuNPs/Pt (c), and MWCNT-AuNP-PDDA-AChE/Pt (d) in 0.1 M KCl containing 5 mM $[Fe(CN)_6]^{3-/4-}$ (1:1) with a frequency range from 100 kHz to 1 Hz with an amplitude of 5 mV.

3. Results and discussion

3.1. Preparation and characterization of MWCNT-AuNP-(PDDA-AChE)n/Pt electrode

Experiments were carried out with the aim of developing a simple and effective AChE/ChOx bienzyme immobilization matrix. Fig. 1 shows the stepwise fabrication process of the AChE/ChOx bienzyme amperometric acetylcholine biosensor. First, a thiolated

MPTMOS sol containing MWCNTs and ChOx was dropped on the surface of a cleaned Pt electrode as the base electrode. MPTMOS is a good conjunction reagent with two reactive functional groups, the trimethoxysilane head group and the thiol tail (Wu et al., 2008). Trimethoxysilane head group can undergo hydrolysis and condensation reaction to form a covalently linked siloxane network which can be used for immobilization of ChOx and MWCNTs. The thiol tail can be used to assemble AuNPs via the Au—S bond. Meanwhile, PDDA-MWCNTs can provide an interface for the assembly of AuNPs and AChE through electrostatic interaction between positively charged PDDA and negatively charged AuNPs and AChE. Second, AuNPs were immobilized on the base electrode through chemisorption and electrostatic attraction. Third, the alternate deposition of PDDA and AChE was on the AuNPs modified base electrode to obtain MWCNT-AuNP-(PDDA-AChE)n/Pt electrode for optimizing AChE loading. Here AChE is used as a negatively charged material for preparing the multilayer films of PDDA-AChE around pH 8.0, because the isoelectric point (pI) of AChE lies around pH 5.0 (Vamvakaki et al., 2008), which can adsorb the polycationic PDDA by electrostatic adsorption.

The typical scanning electron microscope (SEM) images of sol-MWCNTs, sol-MWCNT-AuNPs, and MWCNT-AuNP-PDDA-AChE were characterized by SEM studies (see Supplementary Material Fig. S1). The bare substrate surface is relatively compact and smooth (Fig. S1a). Fig. S1b and c display a stepwise layering of sol-MWCNT and immobilization of AuNPs (the small bright dots) onto the surface, respectively. After the immobilization of AChE, the surface of sol-MWCNT-AuNPs undergoes a drastic change, confirming the successfully self-assembly of AChE onto the sol-MWCNT-AuNPs surface (Fig. S1d). This is further supported by the EIS measurements, as shown in Fig. 2. The EIS includes a semicircular part and a linear part. The semicircular part at higher frequencies corresponds to the electron transfer limited process, while the linear part at lower frequencies corresponds to the diffusion process. The diameter of the semicircle is equivalent to the charge transfer resistance, Rct (Zhu et al., 2010). It is noted that the bare Pt electrode shows a very small Rct (Fig. 2a), indicating a very fast electron-transfer process of $[Fe(CN)_6]^{3-/4-}$. At sol-MWCNTs/pt electrode, an obvious increase in the semicircle diameter is observed (Fig. 2b). This can be explained by the fact that MWCNTs are immobilized in the sol–gel which acts as the inert electron and mass transfer blocking layer (Jia et al., 2002), so sol-bound MWCNTs decrease the ability for MWCNTs to transfer electron. When AuNPs are chemisorbed on the sol-MWCNTs/pt electrode, the semicircle diameter decreases obviously (Fig. 2c), implying that AuNPs are acting as good electron conducting materials. Compared to the sol-MWCNT-AuNPs/pt electrode, the semicircle diameter increases with the self-assembly of AChE (Fig. 2d), confirming the immobilization of enzyme. It may be due to the negatively charged AChE and the increase of the thickness of the interface, which reduced the electron transfer between anionic $[Fe(CN)_6]^{3-/4-}$ and Pt electrode (Du et al., 2008; Yin et al., 2009; Chauhan and Pundir, 2011). Taken together, the SEM images and EIS data showed that AuNPs and AChE were successfully assembled on the thiolated sol-modified electrode surface.

It has been demonstrated that AuNPs with the diameter of 20 nm can be both diffused into and on the surface of the sol–gel network (Bharathi et al., 2001), and the small-sized AuNPs, 25 nm, can form continuous AuNPs film on the surface of the (mercaptopropyl) siloxane monolayer-modified electrode which was more densely packed than the monolayer bound to the large-sized AuNPs (Doron et al., 1995). To further examine the size of AuNPs, the prepared AuNPs sample was observed by TEM and optical spectra measurements, as shown in Fig. 3. The SPR peak of AuNPs was located at about 520 nm (Fig. 3A), the characteristic absorbance of AuNPs, which was confirmed by TEM image of AuNPs (Fig. 3B). The TEM image indicated that AuNPs were almost spherical in shape with

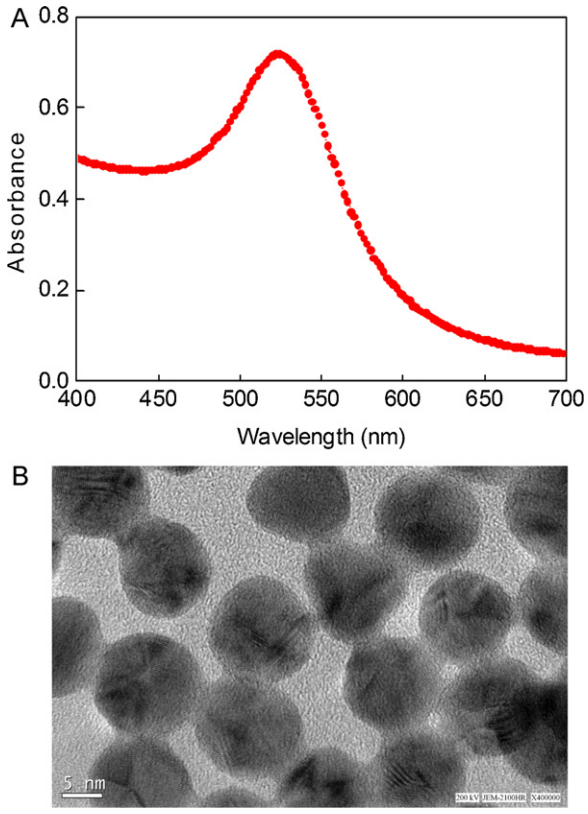

Fig. 3. The UV–Vis absorption spectrum (A) and TEM image (B) of AuNPs.

an average size of about 15 nm. Therefore, both AuNPs and MWCNTs used in this work could be distributed throughout the sol–gel network. They can form a continuous array of AuNPs and MWCNTs on the electrode, providing necessary conduction pathways.

3.2. Electrochemical behaviors of MWCNT-AuNP-(PDDA-AChE)n/Pt electrode

In order to prepare the acetylcholine biosensor, the MWCNT-ChOx/Pt electrode was first prepared as the base electrode, on which AuNPs and PDDA-AChE multilayer films were deposited further. Fig. 4 shows cyclic voltammograms of MWCNT-ChOx (a, b and c), MWCNT-AuNP-PDDA-AChE (A, B and C) modified Pt electrodes in PBS containing no choline and acetylcholine (a and A), 1.6 mM acetylcholine (b and B), and 1.6 mM choline (c and C) in the applied potential range from 0 to 600 mV with a scan rate of 50 mV/s, respectively. The response of both MWCNT-ChOx/Pt electrode and MWCNT-AuNP-PDDA-AChE/Pt electrode in PBS displayed a low background current. Upon addition of 1.6 mM choline, a large oxidation current was observed, confirming that ChOx catalyzed the oxidation reaction of choline and the resultant H_2O_2 was electrooxidized at the electrodes. The current of MWCNT-AuNP-PDDA-AChE/electrode was much higher than that of MWCNT-ChOx/Pt electrode, demonstrating a synergistic effect of MWCNTs and AuNPs, which was in accordance with that reported for nanocomposite modified electrodes (Du et al., 2010; Zhou et al., 2010). As expected, upon addition of 1.6 mM acetylcholine, no current was observed at MWCNT-ChOx/Pt electrode, while MWCNT-AuNP-PDDA-AChE/Pt electrode displayed an obvious oxidation current, which not only proved that AChE was successfully assembled on MWCNT-AuNP-ChOx/Pt electrode, but also proved that two sequential enzyme reactions, the hydrolysis reaction of acetylcholine and an oxidation reaction of resulting choline, can proceed efficiently in the prepared bienzyme immobilization

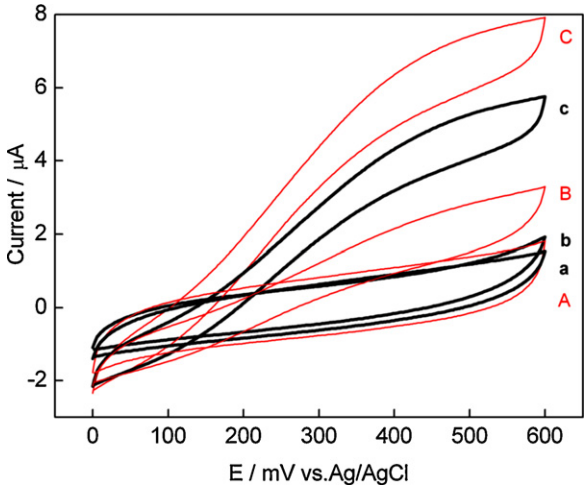

Fig. 4. Cyclic voltammograms of MWCNT-ChOx (a, b and c) and MWCNT-AuNP-PDDA-AChE (A, B and C) modified Pt electrode in PBS containing no choline and acetylcholine (a and A), 1.6 mM acetylcholine (b and B), and 1.6 mM choline (c and C), respectively. The scan rate is 50 mV/s.

matrix. Therefore, we get the ideal structure of the acetylcholine biosensor, as shown in Fig. 1.

The amperometric acetylcholine biosensor originates from the oxidation current of H_2O_2, which is generated during the course of the AChE/ChOx-catalyzed oxidation of acetylcholine in the presence of dissolved oxygen. The performances of the acetylcholine sensor should significantly depend on the relative value of AChE and ChOx loading on the electrode surface (Chen et al., 1998). Here one simplifying assumptions is made. It is assumed that immobilization of ChOx on the electrode is constant and enough since ChOx mainly affects the overall signal, not their relative responses. So this study investigates experimentally the optimum AChE loading. To optimize the loading of AChE on the electrode, the amperometric responses of MWCNT-AuNP-(PDDA-AChE)n/Pt electrodes were studied at the applied potential of 0.6 V vs. Ag/AgCl on successive addition of acetylcholine, which are 0.05, 0.1, 0.2, 0.4, 0.8, and 1.6 mM, respectively, as shown in Fig. 5. Curves 1–3 displayed the amperometric response of 1–3 layers of PDDA-AChE modified MWCNT-AuNP-ChOx/Pt electrode, respectively. Experiments showed that the resulting acetylcholine biosensors exhibited a rapid and sensitive response to the change of acetylcholine concentration. The biosensor achieved 95% of the

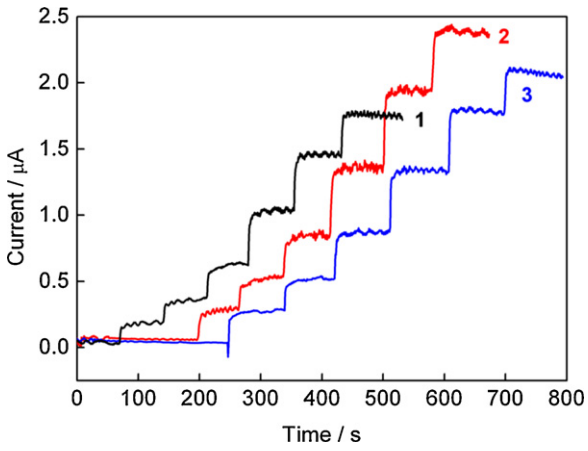

Fig. 5. Amperometric response of different layers of PDDA-AChE multilayer films modified MWCNT-AuNP-ChOx/Pt electrode upon successive addition of acetylcholine at 0.6 V vs. Ag/AgCl (number of multilayer films indicated on graph).

steady-state current within 15 s, which might be due to the easy diffusion of the products of enzymatic reactions in the sol–gel and multilayer films, and the excellent electron-transfer ability of MWCNTs and AuNPs. The amperometric response of the resulting acetylcholine biosensor increased from one to two layers of PDDA-AChE multilayer films, while the response was no longer enhanced by further increasing the number of the PDDA-AChE layer. This might be due to the relative values of catalytic activity of AChE and ChOx (Chen et al., 1998; Shi et al., 2005). The current firstly depends on the rate of the hydrolysis reaction of acetylcholine catalyzed by AChE because of an insufficient loading of AChE. When the electrode was equipped with more than two layers of PDDA-AChE, the current is determined by the rate of the oxidation reaction of choline catalyzed by ChOx. These considerations are qualitatively in accordance with the fact that the catalytic activities of AChE and ChOx used are nominally 1100 units/mg and 17 units/mg, respectively. So among the resulting acetylcholine biosensors, the MWCNT-AuNP-$(PDDA\text{-}AChE)_2$/Pt electrode was best, confirming that the coupling of sol–gel and self-assembly process is suitable and effective for optimizing enzyme loading.

In order to select an adequate operating potential, the effect of applied potential on the current of the MWCNT-AuNP-$(PDDA\text{-}AChE)_2$/Pt electrode was carried out in 0.4 mM acetylcholine at the applied potential shifts from 0.1 to 0.7 V. The results showed that the current increased as the applied potential shifts from 0.1 to 0.35 V, and reached a plateau around 0.35–0.7 V, which was in agreement with that reported for the detection of glucose and choline (Wu et al., 2007b; Qin et al., 2010). Therefore, taking the sensitivity and selectivity into consideration, the applied potential of 0.35 V was chosen as the working potential.

Fig. 6A shows the amperometric response of the MWCNT-AuNP-$(PDDA\text{-}AChE)_2$/Pt electrode on successive addition of acetylcholine in lower concentration regions (a) which are 0.005, 0.01, 0.02, 0.04, 0.08, 0.16 mM, and in higher concentration regions (b), which are 0.05, 0.1, 0.2, 0.4, 0.8, 1.6 mM, respectively. The response current increased with increasing the acetylcholine concentration in the range from 0.005 to 1.6 mM and reached a saturation value at high acetylcholine concentration, indicating that the AChE/ChOx catalytic reaction changed from first to zero order, which was the characteristic of Michaelis–Menten kinetics. The calibration curve under the optimized experimental conditions was shown in Fig. 6B. A good linear relation was observed in the range from 0.005 to 0.4 mM acetylcholine with a correlation coefficient of 0.9955. Linear regression equation (10 points) was $Y(\mu A) = 0.006 + 3.395X$ (acetylcholine, mM) with the detection limit of 1 μM when signal-to-noise ratio was 3. Relative standard deviation was found to be 5% for five successive measurements of 0.1 mM acetylcholine, indicating an acceptable reproducibility. A comparison between the analytical utility of some AChE-based biosensors for acetylcholine was made (see Supplementary Material Table S1). The calibration range of the proposed biosensor is not extremely wide, but it is better than the practical range reported in the literatures (Vamvakaki et al., 2008; Wang et al., 2009; Zhu et al., 2009; Deng et al., 2011). And the detection limit was 1 μM which was lower than that of some other detection methods (Ozturk et al., 2007; Pchelintsev and Millner, 2008; Shimomura et al., 2009; Chen et al., 2011). More importantly, the obvious advantage of this study is simple and effective in optimizing AChE/ChOx loading ratio which is an important criterion for the performance of the bienzyme or multienzyme biosensor.

The selectivity of the acetylcholine biosensor relative to various potentially electroactive species, such as ascorbic acid, uric acid, acetaminophen, dopamine and serotonin was tested in PBS. No noticeable changes in current were detected through measuring the amperometric response to 0.2 mM acetylcholine on successive addition of 0.1 mM ascorbic acid, 0.1 mM acetaminophen, 0.5 mM uric acid, 10 μM serotonin, and 10 μM dopamine at the potential

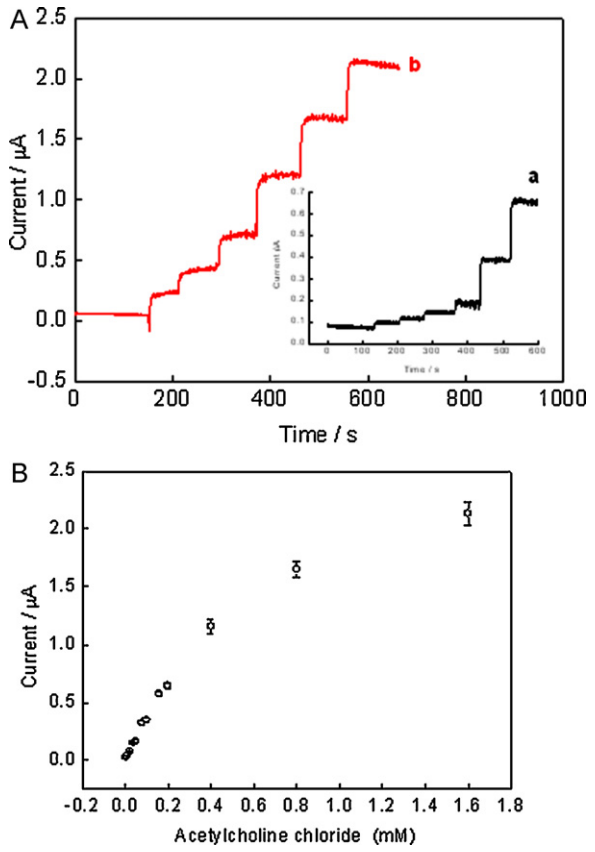

Fig. 6. (A) Amperometric responses of the MWCNT-AuNP-(PDDA-AChE)$_2$/Pt electrode upon successive addition of acetylcholine in the lower (a) and higher (b) concentration regions at 0.35 V vs. Ag/AgCl. (B) The calibration curve of the above electrode. Error bars = ±standard deviation and n = 5.

of 0.35 V vs. Ag/AgCl. The acceptable selectivity of the biosensor could be mainly attributed to the high sensitivity of the resulting acetylcholine biosensor and the relative low working potential for detection. Moreover, it may be due to the MPTMOS sol–gel, which has the good anti-interference ability (Yang et al., 2008).

In order to demonstrate long-term stability, the amperometric response of the MWCNT-AuNP-(PDDA-AChE)$_2$/Pt electrode to 0.1 mM acetylcholine was measured every day. When the electrode was stored at 4 °C for two months, it remained 80% of its initial current response. The high stability should be attributed to the stability of sol–gel and self-assembly films and the natural features of MWCNTs and AuNPs, which can provide a favorable microenvironment for preserving the activity of AChE and ChOx.

4. Conclusions

This paper presents a novel amperometric acetylcholine biosensor based on self-assembly of AuNPs and AChE on the MWCNTs/ChOx/sol–gel-modified Pt electrode surface. Among the resulting biosensors, the biosensor based on two layers of PDDA-AChE showed the best performance, confirming that the coupling of sol–gel and self-assembly process was suitable and effective for optimizing enzyme loading. The proposed acetylcholine biosensor has shown satisfactory results for the determination of acetylcholine such as high sensitivity and long-term stability. Significant advantages of the proposed biosensor include simplicity of fabrication and the benefits of sol–gel, self-assembly, nanoparticles and enzyme-based amperometric biosensor. More importantly, this study can provide a universal and effective immobilization platform for constructing the multienzyme-based biosensor.

Acknowledgments

This research is supported by the National Natural Science Foundation of China (30800261 and 81127001), the Scientific Research Foundation for the Returned Overseas Chinese Scholars, State Education Ministry ([2009]8), the Scientific Research Foundation of the State Human Resource Ministry for Returned Chinese Scholars (2008) and the Department of Education of Guangdong Province (Breeding Program, 2008).

Appendix A. Supplementary data

Supplementary data associated with this article can be found, in the online version, at doi:10.1016/j.bios.2011.12.014.

References

Andreescu, S., Luck, L.A., 2008. Anal. Biochem. 375, 282–290.
Bharathi, S., Nogami, M., Ikeda, S., 2001. Langmuir 17, 1–4.
Chauhan, N., Pundir, C.S., 2011. Anal. Chim. Acta 701, 66–74.
Chen, Q., Kobayashi, Y., Takeshita, H., Hoshi, T., Anzai, J., 1998. Electroanalysis 10, 94–97.
Chen, Z., Ren, X., Meng, X., Chen, D., Yan, C., Ren, J., Yuan, Y., Tang, F., 2011. Biosens. Bioelectron. 28, 50–55.
Deng, L., Zhang, L., Shang, L., Guo, S., Wen, D., Wang, F., Dong, S., 2009. Biosens. Bioelectron. 24, 2273–2276.
Deng, S., Lei, J., Cheng, L., Zhang, Y., Ju, H., 2011. Biosens. Bioelectron. 26, 4552–4558.
Doron, A., Katz, E., Willner, I., 1995. Langmuir 11, 1313–1317.
Du, D., Chen, S., Song, D., Li, H., Chen, X., 2008. Biosens. Bioelectron. 24, 475–479.
Du, D., Chen, W., Zhang, W., Liu, D., Li, H., Lin, Y., 2010. Biosens. Bioelectron. 25, 1370–1375.
Firdoz, S., Ma, F., Yue, X., Daia, Z., Kumar, A., Jiang, B., 2010. Talanta 83, 269–273.
Hill, H., Mikin, C., 2006. Nat. Protoc. 1, 324–336.
Huang, J., Zhang, X., Liu, S., Lin, Q., He, X., Xing, X., Lian, W., Tang, D., 2011. Sens. Actuators B 152, 292–298.
Jia, J., Wang, B., Wu, A., Cheng, G., Li, Z., Dong, S., 2002. Anal. Chem. 74, 2217–2223.
Kannan, P., Abraham John, S., 2010. Anal. Chim. Acta 663, 158–164.
Li, Y., Yuan, R., Chai, Y., Song, Z., 2011. Electrochim. Acta 56, 6715–6721.
Liu, B., Yang, Y.H., Wu, Z.Y., Wang, H., Shen, G.L., Yu, R.Q., 2005. Sens. Actuators B 104, 186–190.
Mackey, D., Killard, A.J., Ambrosi, A., Smyth, M.R., 2007. Sens. Actuators B 122, 395–402.
Minati, L., Torrengo, S., Speranza, G., 2010. Surf. Sci. 604, 508–512.
Mitchell, K.M., 2004. Anal. Chem. 76, 1098–1106.
Ozturk, G., Alp, S., Timur, S., 2007. J. Mol. Catal. B: Enzym. 47, 111–116.
Pchelintsev, N.A., Millner, P.A., 2008. Anal. Chim. Acta 612, 190–197.
Pundir, Chauhan, C.S., Rajneesh, N., Verma, Ravi, M., 2011. Sens. Actuators B 155, 796–803.
Qin, X., Wang, H., Wang, X., Miao, Z., Chen, L., Zhao, W., Shan, M., Chen, Q., 2010. Sens. Actuators B 147, 593–598.
Shen, Y., Wu, T., Zhang, Y., Li, J., 2005. Talanta 65, 481–488.
Shi, H., Zhao, Z., Song, Z., Huang, J., Yang, Y., Anzai, J., Osa, T., Chen, Q., 2005. Electroanalysis 17, 1285–1290.
Shimomura, T., Itoh, T., Sumiya, T., Mizukami, F., Ono, M., 2009. Enzyme Microb. Technol. 45, 443–448.
Tello, A., Cárdenas, G., Häberle, P., Segura, R.A., 2008. Carbon 46, 884–889.
Vamvakaki, V., Hatzimarinaki, M., Nikos Chaniotakis, N., 2008. Anal. Chem. 80, 5970–5975.
Wang, B., Li, B., Deng, Q., Dong, S., 1998a. Anal. Chem. 70, 3170–31740.
Wang, J., Pamidi, P.V.A., Zanette, D.R., 1998b. J. Am. Chem. Soc. 120, 5852–5853.
Wang, X.F., Zhou, Y., Xu, J.J., Chen, H.Y., 2009. Adv. Funct. Mater. 19, 1–7.
Wu, B.Y., Hou, S.H., Yin, F., Li, J., Zhao, Z.X., Huang, J.D., Chen, Q., 2007a. Biosens. Bioelectron. 22, 838–844.
Wu, B.Y., Hou, S.H., Yin, F., Zhao, Z.X., Wang, Y.Y., Wang, X.S., Chen, Q., 2007b. Biosens. Bioelectron. 22, 2854–2860.
Wu, F., Hu, Z., Xu, J., Tian, Y., Wang, L., Xian, Y., Jin, L., 2008. Electrochim. Acta 53, 8238–8244.
Xiao, L., Wildgoose, G.G., Compton, R.G., 2008. Anal. Chim. Acta 620, 44–49.
Yang, Y., Tseng, T., Yeh, J., Chen, C., Lou, S., 2008. Sens. Actuators B 131, 533–540.
Yang, Y., Yang, H.Y., Shen, G.L., Yu, R.Q., 2005. Anal. Chim. Acta 530, 205–211.
Yin, H., Ai, S., Xu, J., Shi, W., Zhu, L., 2009. J. Electroanal. Chem. 637, 21–27.
Zhang, J., Li, J., Yang, F., Zhang, B., Yang, X., 2009. Sens. Actuators B 143, 373–380.
Zhou, K., Zhu, Y., Yang, X., Li, C., 2010. Electroanalysis 22, 259–264.
Zhu, N., Gao, H., Xu, Q., Lin, Y., Su, Y., Mao, L., 2010. Biosens. Bioelectron. 25, 1498–1503.
Zhu, W., An, Y., Zheng, J., Tang, L., Zhang, W., Jin, L., Jiang, L., 2009. Biosens. Bioelectron. 24, 3594–3599.